Kinetics and Activation Parameters for Dyeing of Cellulose-Polyethylene Terephthalate Blends with a Reactive Dye Using a Convenient, Robust Dye Flow-System

Shirley Possidonio, [ORCID] *,[a] Camila S. M. Iar,[a] Luzia P. Novaki[b] and Omar A. El Seoud[b]

[a]*Departamento de Química, Instituto de Ciências Ambientais, Químicas e Farmacêuticas,
Universidade Federal de São Paulo, 09913-030 Diadema-SP, Brazil*

[b]*Instituto de Química, Universidade de São Paulo, 05508-000 São Paulo-SP, Brazil*

Dyeing of cellulose with reactive dyes (RDs) is an important commercial process because the fibers/fabrics have vivid colors with excellent fastness, since the RD is covalently bonded to cellulose. The subject of the present study is dying of cotton-polyethylene terephthalate (PET) blends using a flow system where the RD absorbance is contentiously monitored by UV-Vis spectroscopy. This allows the collection of extensive data points (≥ 300) to calculate the rate constants, hence the corresponding activation parameters. At a fixed pH = 11.2, a pseudo second-order rate law fits the absorbance *vs.* time data satisfactorily. At a constant temperature, the order of the dyeing rate constant (k_2) is higher for the blend containing 88.9% cotton. The dyeing activation energy, on the other hand, is higher for the blend containing 50% cotton. These results were attributed to the adverse effects of (hydrophobic) PET on the diffusion of RD into the blend. We calculated an equation that shows the dependence of k_2 on the temperature and cotton wt.% of the blend.

Keywords: cellulose-PET blends, cellulose dyeing, reactive dyes, dyeing kinetics

Introduction

Dyeing of cellulose (Cel-OH) fibers/textiles by reactive dyes (RDs) is an important industrial process because the products have vivid colors with excellent color fastness. This process occurs via RD physical adsorption onto the fiber/fabric followed, under alkaline conditions, by dye fixation. We employ the latter term to denote the reaction leading to formation of Cel-O-RD covalent bond. Fixation occurs either by an S_N substitution of a leaving group (usually Cl^{-}), Michael addition or, for bifunctional RDs, both mechanisms simultaneously,[1] see Figure 1. In alkaline solutions, dye hydrolysis is the main side reaction, see Figure 1.[2,3]

In addition to alkali, dyeing is carried out in the presence of an electrolyte, e.g., NaCl or Na$_2$SO$_4$, whose role is to promote an even dye uptake by the fiber/fabric. In addition to induced RD aggregation and reduced solubility in the aqueous bath, the added electrolyte screens the repulsive forces between the anionic RD and the negatively charged cellulosic surface.[4,5] The alkaline condition (pH > 11)

is required to generate the so called "alkali-cellulose", Cel-O[-],[3] that is much more nucleophilic than Cel-OH, thus causing RD fixation.

The dyeing processes are usually experimentally followed by withdrawing samples from the dyeing bath, measuring the absorption of the remaining dye, e.g., by UV-Vis spectroscopy, followed by calculation of the corresponding rate constant. Because of the slowness of this protocol, the number of experimental points employed to calculate the rate constants is usually inconveniently small. Examination of 27 publications on the kinetics of dyeing revealed that the rate constants were calculated using ≤ 20 data points, see Figure 2. As discussed elsewhere in detail,[6] the number of data points, the time intervals between the data points, and the number of half-lives monitored are crucial parameters that bear on the accuracy of the calculated rate constants. Therefore, the values of many dyeing rate constants in the literature should be considered with some reserve because they were based on an inadequate number of data points.

In order to remedy this situation, we decided to use a different experimental setup where the RD concentration in the bath is monitored continuously using a home-constructed dye flow system that permits obtaining a large

*e-mail: possidonio@unifesp.br
Editor handled this article: Fernando C. Giacomelli (Associate)
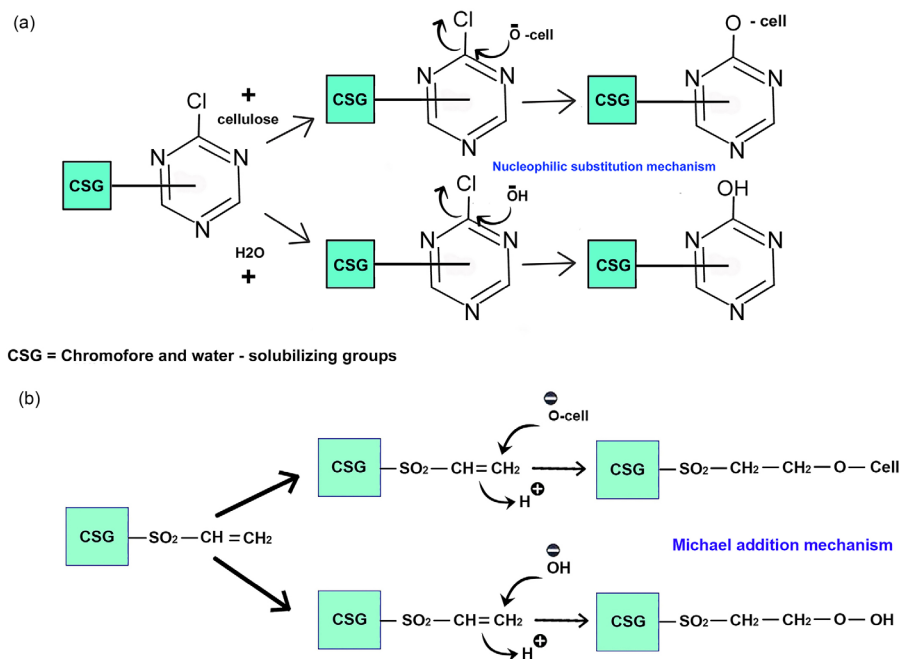
Figure 1. (a) Nucleophilic substitution and (b) Michael addition mechanisms of reactive dye fixation onto cellulose fibers/fabrics.
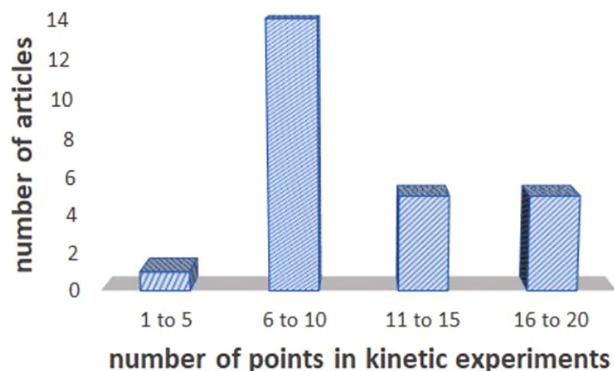
Figure 2. Number of experimental points in published articles on dyeing kinetics or dye adsorption kinetics in wastewater treatment: (1 to 5 points);[7] (6 to 10 points);[8-25] (11 to 15);[1,23-27] (16 to 20 points).[28-32]

number of experimental data points (typically ≥ 300 points), thus allowing accurate calculation of the dyeing rate constants (k_2).

Performing chemical kinetics in a flow system offers advantages, in addition to obtaining accurate rate data: it eliminates contact with potentially harmful chemicals; it largely reduces the consumption of reagents and solvents, and it generates much less waste.[33] Surprisingly, however, such systems were rarely used in the kinetic study of fabric dyeing.[34]

The use of so called poly cotton, a blend of cotton and polyethylene terephthalate (PET), is increasing worldwide, because of the fabric excellent mechanical properties, lower price relative to pure cotton, and suitability for use in warm weather.[35,36] Depending on the end use, these blends have variable contents of PET. It is important, therefore, to know how the kinetics of dyeing the cotton part, e.g., with reactive dyes depends on the biopolymer content. To our knowledge, this information is not available, although there is extensive data on the kinetics of dyeing of pure cotton and pure PET. To remedy this situation, we carried out the present study to determine the dependence of dyeing kinetic data of these blends on their cotton content.

We dyed blends containing 50 and 88.9 wt.% cotton (hereafter designated as B50 and B89, respectively) because these are extensively used commercially. To calculate the dyeing activation parameters, we studied the process at four different temperatures (T). As the dyeing bath is open, we used temperatures lower than those used industrially to avoid water evaporation, leading to changes in species concentrations. Note that cotton, but not PET, is dyed by the reactive dye, hence values of the rate constants, and the corresponding activation parameters depend on the cotton wt.% in the blend. Based on our results, we calculated an equation that correlates the values of k_2 with T and the cellulose wt.% in the blend. This equation can be employed (applying the appropriate statistical protocol) to predict the rate constants under a variety of experimental conditions, thus saving time, labor and material.

Experimental

Materials

All reagents and solvents were purchased from Sigma-Aldrich or Synth (São Paulo, Brazil) and were purified as

given elsewhere.[37] The B50 and B89 fabrics were kindly supplied by Prof Regina A. Sanches, of EACH-USP, and were treated before dyeing in a solution of Tween 80 nonionic surfactant (3 g L^{-1}) and Na$_2$CO$_3$ (5 g L^{-1}), for 2 h at 80 °C, followed by washing with water and drying at room temperature. C.I. Reactive Dye 195 (Ovecrom red 3BS) (RD) (Figure 3) was kindly provided by OV Chemicals (São Paulo, Brazil) and was used without purification.
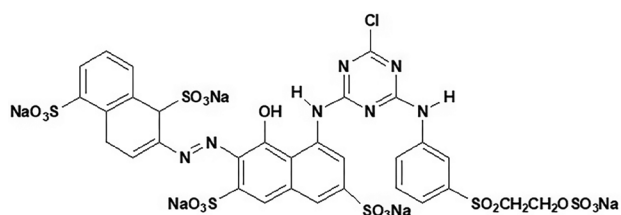
Figure 3. Molecular structure of C.I. Reactive Dye 195.

Experimental setup for studying the kinetics of poly cotton dyeing

Sodium sulfate solution (250 mL; 0.25 wt.%) was placed into a tall-form beaker and thermostated at the required temperature (15, 25, 35 and 45 °C; Lauda RP245E thermostat, Lauda-Konigshofen, Germany) using slow mechanical agitation. The B50 or B89 blend (6.25 g) was introduced into the electrolyte solution. After 30 min, 2 mL of RD solution (0.09 mmol L^{-1}) were added, followed by 12.5 g of solid Na$_2$CO$_3$ with agitation; the final solution pH was 11.2 (Metrohm 827 pH lab pHmeter, Herisau, Switzerland).

A home-constructed flow system was employed to pump/circulate the dye solution from the dyeing bath into a flow-cell inserted into a thermostated cuvette holder of a Shimadzu UV-2550 UV-Vis (Kyoto, Japan) spectrophotometer, see Figure 4. The experimental setup is as follows: the solution was withdrawn from the dyeing bath (beaker) by a peristaltic pump (Ismatec, REGLO, Glattbrugg, Switzerland) at a flow rate of 5-10 µL min^{-1}. The latter solution was continuously diluted with water, using a Y-shaped glass mixing chamber (dilution ratio was adjusted to obtain suitable absorbance values between 0.2 and 1.0) and then pumped (0.7 mL min^{-1}) into a 1 cm pathlength flow cell (Starna 583.4.14-Q-10/Z15, Atascadero, USA), using a second peristaltic pump (Cole-Parmer, Masterflex 7523-80, Chicago, USA). The dye absorbance was registered continuously at 544 nm as a function of time until the difference between two successive measurements, 2 min apart was < 0.05. After dye absorbance measurement, the solution in the flow-cell was discarded properly. All runs were carried out in duplicate.

Calculation of dyeing rate constants

All dye concentrations were calculated from a Beer's law plot between absorbance and dye concentration ((dye) = 4.4 × 10^{-6} to 3.5 × 10^{-5} mol L^{-1}; ε = 30194 L mol^{-1} cm^{-1}; correlation coefficient of Beer's law plot = 0.9992, at λ_{max} = 544 nm).

As shown elsewhere,[8,38] this dyeing is a pseudo second order reaction whose rate constant (k_2; g mg^{-1} s^{-1}) is calculated from a plot of the dependence of dye concentration that is fixed on cellulose (q_t, mg dye *per* g cotton), as a function of time. The former concentration is calculated from equation 1:
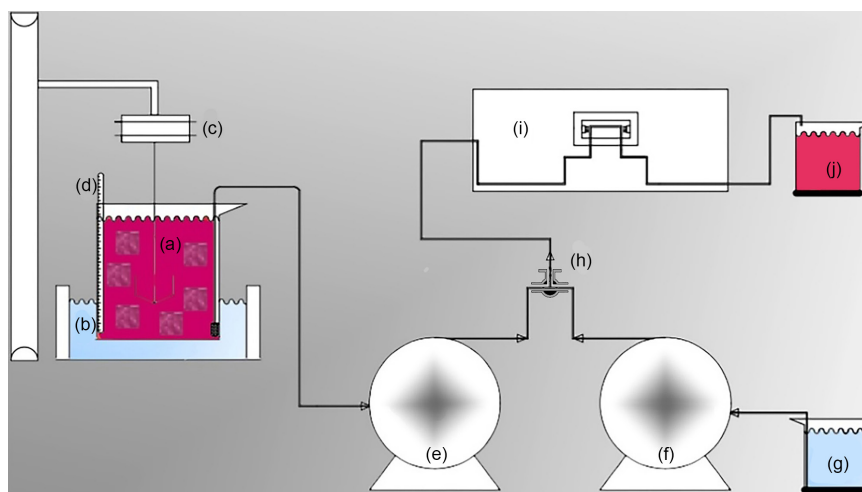
Figure 4. Scheme for the home-constructed flow system: (a) fabric blend in the alkaline dye solution; (b) thermostat for the dyeing bath; (c) mechanical stirrer; (d) thermometer; (e) first peristaltic pumps for solution removal from the dyeing bath at a rate of (0.5 µL min^{-1}); (f) second peristaltic pumps for solution dilution by water from a beaker (g). Dilution valve for the dye solution (h). The diluted dye solution was then pumped at a rate of (0.7 mL min^{-1}) into the flow-cell, (i) inserted into the themostated cell holder of the UV-Vis spectrophotometer. After the measurement, the dye solution in the flow cell is discarded (j).

J. Braz. Chem. Soc. **2024**, *35*, 2, e-20230129

3 of 7

$$q_t = \frac{(C_0 - C_t)V}{m} \qquad (1)$$

where, C_0 and C_t are the initial dye concentration and that at time t, respectively (g mL^{-1}); V is the volume of dye solution (mL) and m represents the cotton mass (g) in the fabric blend. The pseudo-second-order expression is given by equation 2, where q_e and k_2 were calculated, respectively, from the slope and intercept of a plot of t/q_t *versus* t.[9]

$$\frac{t}{q_t} = \frac{1}{k_2 q_e^2} + \frac{1}{q_e}t \qquad (2)$$

In equation 2, q_e and q_t express the concentration of dye fixed on cellulose (mg dye *per* g cellulose) at end of dyeing (i.e., "infinity" value), and at a given time t, respectively; k_2 was defined previously.

The reaction activation parameters were calculated from the values of k_2 by the standard equations 3 to 6:[8]

$$\ln k_2 = \ln A - \frac{E_a}{RT} \qquad (3)$$

where A is the Arrhenius factor (min^{-1}), E_a the activation energy (kJ mol^{-1}), R the universal gas constant (8.314 J mol^{-1} K^{-1}) and T the absolute temperature in Kelvin.

Activation enthalpy (ΔH^*, kJ mol^{-1}), activation entropy (ΔS^*, J mol^{-1} K^{-1}) and activation Gibbs free energy (ΔG^*, kJ mol^{-1}) of dyeing were then estimated according to the expressions:

$$E_a = \Delta H^* + RT \qquad (4)$$

$$\Delta G^* = -RT\ln\left(\frac{k_2 h}{k_B T}\right) \qquad (5)$$

$$\Delta S^* = \frac{\Delta H^* - \Delta G^*}{T} \qquad (6)$$

where (h and k_B) are Planck and Boltzman constant, respectively.

Statistical analysis

We fitted a linear model to the kinetic data using Statistica software version 13.0.[39]

Results and Discussion

Stages of cellulose dyeing

The dyeing process consists of transferring the dye from the solution to the interior of the Cel fiber is complex and involves a sequence of, at least, 3 steps: (*i*) diffusion of the dye from solution to the diffusional boundary layer present on fiber surface, and to the fiber itself; (*ii*) adsorption of the dye on the fiber surface and, finally (*iii*) dye diffusion within the fiber interior (rate determining step). In the case of RDs, after this last stage, the dye is fixed onto the fiber by covalent bonds. It should be noted that any of the three stages may influence the overall dyeing rate constant.[5]

Figure 5a shows the dyeing profile of cotton at 45 °C, at pH 4.75 (50 mmol acetate buffer). The only event that occurs when the blend is immersed into the RD bath is dye physical adsorption (migration phase). This is evident from the UV-Vis absorption trace recorded. As can be seen, the initial absorbance decreases to reach an equilibrium value (ca. 1 h) after which it remains practically constant. After adding Na$_2$CO$_3$ to the dyeing bath, the absorbance decreases fast due to RD fixation that removes RD from the bath (fixation phase).

As indicated above, RD hydrolysis is a parallel reaction. As Figure 5b shows, the solution absorbance in the absence
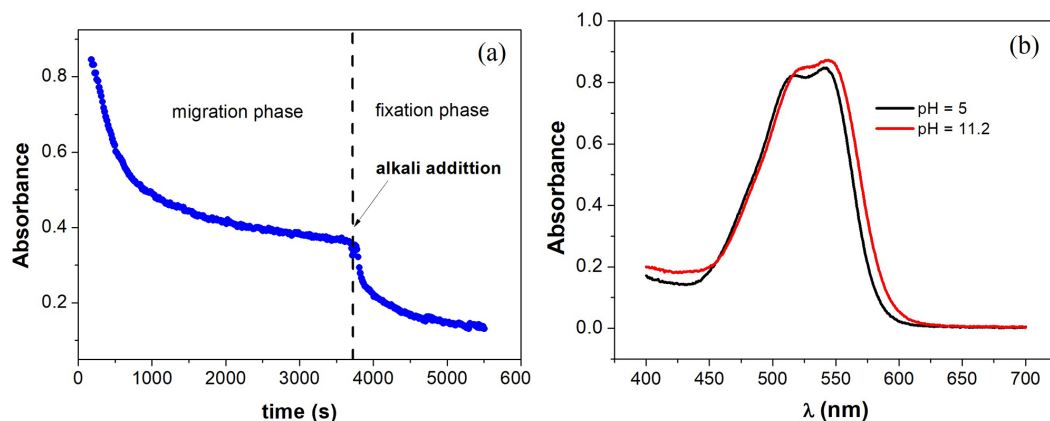
Figure 5. (a) Blend dyeing profile at 45 °C; (b) UV-Vis spectrum of C.I. Reactive Dye 195 at pH = 5 and 11.2.

of the fabric changes very little, although the dye undergoes hydrolysis. The reason is that the chromophoric systems of the original- and hydrolyzed dyes are similar, leading to similar values of λ_{max} and ε_{max}. In summary, the relevant points regarding Figure 5 are: (*i*) the absorbance decrease observed in Figure 5a is due to RD fixation, (*ii*) any discussion about RD exhaustion from the dyeing bath can be deceptive. The reason is that such discussion is based on changes of solution absorbance, which is the sum of the (similar) absorbances of the remaining- and hydrolyzed RD. Consequently, discussing "effective" exhaustion of the dyeing bath is meaningful if the rate of Cel dyeing by the RD is much faster than the rate of RD hydrolysis.

Kinetics of RD fixation

Figures 6a-6c show examples of the data obtained using this flow system; the calculated values of k_2 are based on ≥ 300 data points.
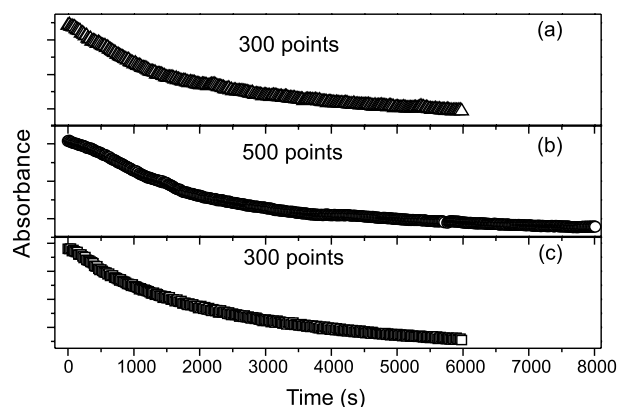
Figure 6. Plots of absorbance *versus* time for: (a) B89 at 45 °C; (b) B50 at 45 °C; (c) B89 at 35 °C.

It is customary to fit different rate laws to the absorbance *vs.* time data and chose the kinetic model that gives the best fit. At the outset, this reaction is 3rd order,

first order in the substrate (cellulose), the dye, and the base because the latter is involved in the generation of Cel-O$^-$, the active species that reacts with RD. Applying a pseudo first-order rate-low is only meaningful if: (*i*) the experiment was carried out under the pseudo-first-order conditions, i.e., the concentrations of system components, except one, are in excess (≥ 10 times that of the reactant of lowest concentration); (*ii*) the rate constant is employed to calculate higher order rate constant. This fundamental aspect is usually not clearly addressed.

At constant pH, the reaction is pseudo-second order (Figure 7) and the rate constants are calculated as given in the Experimental section, with the proviso that their units are given *per* g of Cel. Because RD is not fixed on PET, the rate constants for the blends were calculated based on their Cel-OH wt.%. Table 1 shows the values of the rate constants for cotton/PET blends and the corresponding activation parameters.
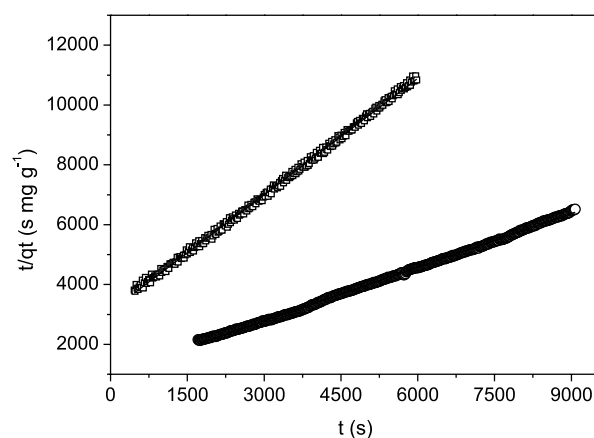
Figure 7. Plot of pseudo-second-order kinetics for: B50 at 45 °C (○); B89 at 35 °C (□).

Figure 7 shows clearly that dyeing of cotton/PET blends by RD obeys pseudo-second order kinetics. Similar plots under other experimental conditions are shown in

Table 1. Pseudo-second order kinetic parameters for cotton/PET dyeing with RD

Parameter[a,b]	Blend							
	B50				B89			
Temperature / °C	15	25	35	45	15	25	35	45
k_2 (10^{-4}) / (g mg^{-1} s^{-1})	0.66	0.97	1.52	2.22	6.73	8.15	8.78	10.6
r^2	0.994	0.996	0.967	0.996	0.999	0.998	0.998	0.992
Ea* / (kJ mol^{-1})		31.1				12.0		
ΔH^* / (kJ mol^{-1})		28.6				9.6		
ΔS^* / (J mol^{-1} K^{-1})		−225.3 (TΔS^* = −67.2 kJ mol^{-1})				−272.5 (TΔS^* = −81.2 kJ mol^{-1})		
ΔG^* / (kJ mol^{-1})		95.8				90.1		

[a]Activation parameters were calculated at 25 °C; [b]the uncertainties are ± 1, 2 and 1 kJ mol^{-1} in ΔH^* (activation enthalpy), ΔG^* (activation Gibbs free energy), and TΔS^* (activation entropy), respectively. k_2: dyeing rate constant; Ea*: activation energy; r^2: correlation coeficient.

J. Braz. Chem. Soc. **2024**, *35*, 2, e-20230129

5 of 7

Figure S1 (Supplementary Information (SI) section). For these plots, all values of r^2 (except B50 at 35 °C) are > 0.99, which validates the pseudo-second order kinetic model.[15] Although the values of Ea* are in the range reported in the literature (8.4-83.7 kJ mol^{-1}),[40] there is a clear dependence on blend composition. This dependence is probably due to the fact that the rate of dyeing is also affected by (anionic) dye diffusion that is slower in PET relative to cellulose, due to the hydrophobic character of the synthetic polymer.[5] Therefore, although there is no RD fixation on PET, the presence of this polymer in the blend can still affect the dependence of k_2 on T, hence the value of Ea*, given the difficulty of diffusion of the dye to into PET. This difficulty increases as a function of increasing the wt.% of PET in the blend, in agreement with the data of Table 1. Regarding the other activation parameters, the negative values of $\Delta S*$ agree with the associative process between the dye and the fiber.

We employed the kinetic data of Table 1 to calculate the regression equation 7 that correlates the values of k_2 with the experimental variables temperature (T) and cotton wt.% in the blend (C). Although the experiments were not carried out according to the design of experiment (DOE) protocol,[41] we plan to use the DOE approach in order to secure a more statistically robust equation for the dependence of k_2 on the experimental variable which allows prediction of the results under a wide range of conditions, thus saving time, labor, and material.

$$k_2 = -1.18 \times 10^{-3} + 1.3 \times 10^{-5}T + 1.8 \times 10^{-5}C \qquad (7)$$

Conclusions

We used a home-constructed flow system to study the kinetics of dyeing cotton-PET blends. The use of this system noticeably increases the accuracy of the calculated rate constants and the corresponding activation parameters, in addition to saving labor. As expected, a pseudo second-order rate law fits the experimental data satisfactorily. At a constant temperature, the order of k_2 is B89 > B50, whereas that of the activation energy is B89 < B50. These results were attributed to the adverse effects of (hydrophobic) PET on the diffusion of (anionic) RD into the blend. As expected, the RD-blend interaction is associated with negative values of $\Delta S*$. An equation that correlates the values of k_2 with T and C (at a constant pH) was calculated. The novelty of the present work is that the flow system makes it feasible to obtain reliable kinetic data that can be employed (applying the appropriate statistical protocol, e.g., DOE) to predict the rate constants under a variety of experimental conditions, thus saving time, labor and material.

Supplementary Information

Acknowledgments

References

1. Lewis, D. M.; *Color. Technol.* **2014**, *130*, 382. [Crossref]

2. Stead, C. V. In *Reactive Dyes in Protein and Enzyme Technology*, vol. 20, 1st ed.; Clonis, Y. D.; Atkinson, T.; Bruton, C. J.; Lowe, C. R., eds.; The Macmillan Press Ltd: London, UK, 1988.

3. Blackburn, R. S.; Burkinshaw, S. M.; *Green Chem.* **2002**, *4*, 47. [Crossref]

4. Burkinshaw, S. M.; Salihu, G.; *Dyes Pigm.* **2019**, *161*, 628. [Crossref]

5. Burkinshaw, S. M.; *Physico-Chemical Aspects of Textile Coloration*, 1st ed.; Filarowski, A., ed.; Society of Dyers and Colorists and John Wiley: Bradford, UK, 2016.

6. El Seoud, O. A.; Baader, W. J.; Bastos, E. L. In *Encyclopedia of Physical Organic Chemistry*, vol. 5; Wang, Z., ed.; John Wiley & Sons: New Jersey, 2017, ch. 8, p. 369.

7. Reddy, N.; Thillainayagam, V. A.; Yang, Y.; *Ind. Eng. Chem. Res.* **2011**, *50*, 5642. [Crossref]

8. Kale, R. D.; Potdar, T.; Gorade, V.; *Sustainable Environ. Res.* **2019**, *29*, 7. [Crossref]

9. Ho, Y. S.; McKay, G.; *Process Biochem.* **1999**, *34*, 451. [Crossref]

10. Vassileva, V.; Valcheva, E.; Zheleva, Z.; *Z. Zheleva J. Univ. Chem. Technol. Metall.* **2008**, *43*, 323. [Link] accessed in July 2023

11. Hamdaoui, M.; Lanouar, A.; *Indian J. Fibre Text. Res.* **2014**, *39*, 310. [Crossref]

12. De Vries, T. S.; Davies, D. R.; Miller, M. C.; Cynecki, W. A.; *Ind. Eng. Chem. Res.* **2014**, *53*, 9686. [Crossref]

13. Farzana, N.; Uddin, M. Z.; Haque, M. M.; Haque, A. N. M. A.; *J. Nat. Fibers* **2020**, *17*, 986. [Crossref]

14. Suteu, D.; Malutan, T.; Bilba, D.; *Desalination* **2010**, *255*, 84. [Crossref]

15. Yi, S.; Dong, Y.; Li, B.; Ding, Z.; Huang, X.; Xue, L.; *Color. Technol.* **2012**, *128*, 306. [Crossref]

16. Dash, S.; Chaudhuri, H.; Gupta, R.; Nair, U. G.; *J. Environ. Chem. Eng.* **2018**, *6*, 5897. [Crossref]

17. Geethakarthi, A.; Phanikumar, B. R.; *Int. J. Environ. Sci. Technol.* **2011**, *8*, 561. [Crossref]

18. Aksu, Z.; Ertuğrul, S.; Dönmez, G.; *J. Hazard. Mater.* **2009**, *168*, 310. [Crossref]

19. de Oliveira Brito, S. M.; Cordeiro, J. L. C.; da Cunha Ramalho, L.; Oliveira, J. F. R.; *SN Appl. Sci.* **2019**, 1226. [Crossref]

20. Ho, Y. S.; McKay, G.; *J. Environ. Sci. Health, Part A: Toxic/Hazard. Subst. Environ. Eng.* **1999**, *34*, 1179. [Crossref]

21. Matyjas, E.; Blus, K.; Rybicki, E.; *Fibres Text. East. Eur.* **2003**, *11*, 66. [Link] accessed in July 2023

22. Ke, G.; Chen, S.; Zheng, Y.; Zhao, Z.; Tang, J.; Peng, F.; *J. Nat. Fibers* **2022**, *19*, 4583. [Crossref]

23. Wang, J.; Gao, Y.; Zhu, L.; Gu, X.; Dou, H.; Pei, L.; *Polymers* **2018**, *10*, 1030. [Crossref]

24. Pei, L.; Liu, J.; Gu, X.; Wang, J.; *J. Text. Inst.* **2020**, *111*, 925. [Crossref]

25. Tam, K. Y.; Smith, E. R.; Booth, J.; Compton, R. G.; Brennan, C. M.; Atherton, J. H.; *J. Colloid Interface Sci.* **1997**, *186*, 387. [Crossref]

26. Chairat, M.; Rattanaphani, S.; Bremner, J. B.; Rattanaphani, V.; *Dyes Pigm.* **2008**, *76*, 435. [Crossref]

27. Tang, B.; Yao, Y.; Chen, W.; Chen, X.; Zou, F.; Wang, X.; *Dyes Pigm.* **2018**, *148*, 224. [Crossref]

28. Subramani, S. E.; Thinakaran, N.; *Process Saf. Environ. Prot.* **2017**, *106*, 1. [Crossref]

29. Dikmen, S.; Gunay, A.; Ersoy, B.; Erol, I.; *Environ. Eng. Manage. J.* **2015**, *14*, 1097. [Crossref]

30. Haque, A. N. M. A.; Hussain, M.; Siddiqa, F.; Haque, M. M.; Islam, G. M. N.; *Tekstilec* **2018**, *61*, 76. [Crossref]

31. Haque, A. N. M. A.; Hussain, M.; Smriti, S. A.; Siddiqa, F.; Farzana, N.; *Tekstilec* **2018**, *61*, 27. [Crossref]

32. Haji, A.; Bidoki, S. M.; Gholami, F.; *Fibers Polym.* **2020**, *21*, 2547. [Crossref]

33. Moreira, B. C. S.; Takeuchi, R. M.; Richter, E. M.; Santos, A. L.; *Quim. Nova* **2014**, *37*, 1566. [Crossref]

34. Lis, M. J.; Maesta Bezerra, F.; Meng, X.; Qian, H.; Immich, A. P.; *World J. Text. Eng. Technol.* **2019**, *5*, 97. [Link] accessed in July 2023

35. Future Market Insights, https://www.futuremarketinsights.com/reports/poly-cotton-fabric-market, accessed in July 2023.

36. Biz Vibe, https://blog.bizvibe.com/blog/textiles-and-garments/5-poly-cotton-advantages-and-disadvantages, accessed in July 2023.

37. Armarego, W. L. F.; *Purification of Laboratory Chemicals*, 8th ed.; Butterworth-Heinemann: Oxford, UK, 2017.

38. Pei, L.; Liu, J.; Cai, G.; Wang, J.; *Text. Res. J.* **2017**, *87*, 2368. [Crossref]

39. *Statistica*, version 13; TIBCO Software Inc., Palo Alto, CA, USA, 2017.

40. Saha, P.; Chowdhury, S. In *Thermodynamics*; Tadashi, M., ed.; IntechOpen: London, 2011.

41. Lendrem, D.; Owen, M.; Godbert, S.; *Org. Process Res. Dev.* **2001**, *5*, 324. [Crossref]

J. Braz. Chem. Soc. **2024**, *35*, 2, e-20230129

7 of 7